# Relativistic *R* matrix and continuum shell model

J. Grineviciute and Dean Halderson

*Department of Physics, Western Michigan University, Kalamazoo, Michigan 49008, USA*

**Background:** The *R* matrix formalism of Lane and Thomas has proven to be a convenient reaction theory for solving many-coupled-channel systems. The theory provides solutions for bound states, scattering states, and resonances for microscopic models in one formalism.

**Purpose:** The first purpose is to extend this formalism to the relativistic case so that the many-coupled-channel problems may be solved for systems in which binary breakup channels satisfy a relative Dirac equation. The second purpose is to employ this formalism in a relativistic continuum shell model.

**Methods:** Expressions for the collision matrix and the scattering amplitude, from which observables may be calculated, are derived. The formalism is applied to the $1p$-$1h$ relativistic continuum shell model with an interaction extracted from relativistic mean-field theory.

**Results:** The simplest of the $\sigma + \omega + \rho$ exchange interactions produces a good description of the single-particle energies in $^{16}$O and $^{90}$Zr and a reasonable description of proton scattering from $^{15}$N.

**Conclusion:** The development of a calculable, relativistic *R* matrix and its implementation in a $1p - 1h$ relativistic continuum shell model provide a simple relatively self-consist physically justifiable model for use in knockout reactions.

## I. INTRODUCTION

The *R* matrix formalism of Lane and Thomas [1] has proven to be the most physical and convenient reaction theory for solving many-coupled-channel systems in light- and medium-mass nuclei. It is not uncommon to couple 30 or more residual states of the target in nonrelativistic calculations, and new computer codes need not be written each time states are added. Microscopic models and nonlocal potentials are easily incorporated in the theory. In addition to providing scattering states, the formalism yields bound states and resonances. Coupled-channel techniques, which involve integrating coupled differential equations, can become unstable for large numbers of channels, and they can miss narrow resonances because the equations must be solved for each energy over the resonance. Also, scattering observables are calculated quickly at a given energy in the *R* matrix formalism because they require diagonalizing matrices whose dimensions are just the number of channels. Additional advantages may be found in a review paper by Descouvemont and Baye [2] and applications in a review in Ref. [3].

This paper is the last of a series of three papers that describe the extension of the *R* matrix theory to the relativistic case so that the many-coupled channels problem may be solved for systems in which binary breakup channels satisfy a relative Dirac equation. The first paper [4] demonstrated that a *R* matrix theory exists for the Dirac equation and derived the appropriate Bloch operator. Then, an example was given for 35.5-MeV neutron scattering from a Woods-Saxon potential. The expansion basis consisted of the free-particle Dirac solutions whose upper components were zero at twice the *R* matrix radius.

Paper [5] demonstrated that Dirac oscillator wave functions [6,7] provided an excellent and convenient expansion basis. This paper also demonstrated that the *R* matrix formalism allows one to easily orthogonalize scattering solutions to

bound-state solutions and to treat nonlocal potentials; and, hence, to calculate exchange terms in relativistic impulse approximation exactly. Examples were given for 160–200-MeV elastic proton scattering from $^{16}$O, $^{40}$Ca, and $^{90}$Zr in the impulse approximation with the two-nucleon *t* matrix elements of Ref. [8]. In Ref. [5], it was shown that the common local-density approximation for the exchange terms was inadequate in relativistic calculations. The discrepancy between the exact and the local-density approximation calculations was traced to the extreme difference between the matrix elements of the negative energy states of the basis functions and, hence, was a relativistic effect.

The present paper provides derivations of the collision matrix expression for coupled channels and the scattering amplitude from which scattering observables can be extracted. As an example of the formalism, relativistic continuum Tamm-Dancoff approximation (TDA) calculations for $^{16}$O are performed with interactions derived from relativistic mean-field theory. Specifically, the formalism referred to as quantum hydrodynamics (QHD) [9] is employed. The classical meson fields of the original QHD are replaced by one-meson exchange potentials. The validity of this replacement is checked by comparing single-particle energies (SPEs) for $^{90}$Zr, calculated from both treatments with the same coupling constants. Surprising agreement is found between the two procedures with the simple $\sigma + \omega + \rho$ exchange. In addition, the simple $\sigma + \omega + \rho$ exchange with QHD coupling constants provides reasonable agreement with experimental $^{15}$N $(p,p)$ $^{15}$N cross sections at 39.84 MeV. This is, therefore, a simple, physically justifiable interaction for later use in knockout reactions. The importance of coupled-channel solutions in $(e,e'x)$ was emphasized in Ref. [10]. Finally, the role of pions is investigated. It is found that pions have a significant effect on SPEs and the $^{15}$N $+ p$ cross section, however, a definitive conclusion on their utility awaits a better

approximation for the matrix elements with pseudovector $\pi N$ coupling.

## II. *R* MATRIX FORMALISM

Solutions to the one-channel Dirac equation will be written in the two-component form

$$u_D = \begin{pmatrix} [F(r)/r]\Phi_{\kappa m} \\ [iG(r)/r]\Phi_{-\kappa m} \end{pmatrix} \tau, \tag{1}$$

where

$$\Phi_{\kappa m} = \sum_{m_\ell m_s} C^{l1/2j}_{m_l m_s m} Y_{lm_l}(\theta, \phi) \chi_{m_s}, \tag{2}$$

where $j = |\kappa| - \frac{1}{2}$ and $\ell = \kappa$ for $\kappa > 0$ but $\ell = -(\kappa + 1)$ for $\kappa < 0$ and $\tau$ indicates a proton or neutron. The regular and irregular Dirac-Coulomb functions are generated as given by Young and Norrington [11] employing the code COULCC [12], and they are given the asymptotic form

$$F_R = \sqrt{E + m} \, \sin \, \phi(r) \quad \text{and} \quad G_R = \sqrt{E - m} \, \cos \, \phi(r),$$

$$F_{IR} = \sqrt{E + m} \, \cos \, \phi(r) \quad \text{and} \quad G_{IR} = -\sqrt{E - m} \, \sin \, \phi(r),$$

where $\varphi(r) = kr + y \log 2kr + \delta'_\kappa - \ell\pi / 2$, $k$ is the momentum of the proton in the center-of-momentum system, $y = Ze^2 E/k$, $E^2 = m_p^2 + k^2$, $\delta'_\kappa = \Psi - \arg \, \Gamma(\gamma + iy) + \frac{\pi}{2}(l + 1 - \gamma)$, $e^{2i\Psi} = \frac{iZe^2/k - \kappa}{\gamma + iy}$, and $\gamma = (\kappa^2 - Z^2 e^4)^{1/2}$. Throughout this paper, $c = \hbar = 1$. Incoming and outgoing waves are constructed as

$$F_I = F_{IR} - iF_R \quad \text{and} \quad G_I = G_{IR} - iG_R \text{ making up } I_c,$$

and

$$F_O = F_{IR} + iF_R \quad \text{and} \quad G_O = G_{IR} + iG_R \text{ making up } O_c,$$

where $c$ indicates a particular channel, $|lj\kappa\tau, J_A(J_B)\rangle$, $J_A$ is the target spin, and $J_B$ the total angular momentum. A wave function with unit outgoing flux is $O_c/\sqrt{2k_c}$.

The appropriate modifications for expanding the one-channel case, given in Ref. [5], to the many-channel case are as follows. The wave function is expanded within the channel radius as $\psi = \sum_\lambda A_\lambda |\lambda\rangle$. The set of $|\lambda\rangle$ will be Dirac oscillators coupled to the spin of the target. The Hamiltonian to be solved is

$$\sum_{\lambda'} \left[ \langle\lambda|H - E|\lambda'\rangle + \sum_c \gamma_{\lambda c}(b_{\lambda'c} - b_c)\gamma_{\lambda'c} \right] A_{\lambda'} = 0, \tag{3}$$

where

$$b_c = G_c(a_c)/F_c(a_c), \tag{4}$$

$$b_{\lambda c} = G_{\lambda c}(a_c)/F_{\lambda c}(a_c), \tag{5}$$

and

$$\gamma_{\lambda c} = F_{\lambda c}(a_c). \tag{6}$$

$G_c$ and $F_c$ are the components of the physical wave function in channel $c$. The theory is placed in calculable form in the

method of Philpott [13] in which one finds a transformation $T$ such that

$$\sum_{\lambda\lambda'} T_{\lambda\mu} [\langle\lambda|H|\lambda'\rangle + \sum_c \gamma_{\lambda c} b_{\lambda'c} \gamma_{\lambda'c}] T_{\lambda'\mu'} = E_\mu \delta_{\mu\mu'}. \tag{7}$$

With this transformation, Eq. (3) becomes

$$\sum_{\mu'} [(E_\mu - E)\delta_{\mu\mu'} - \sum_c \gamma_{\mu c} b_c \gamma_{\mu'c}] A_{\mu'} = 0, \tag{8}$$

where $\gamma_{\mu c} = \sum_\lambda \gamma_{\lambda c} T_{\lambda\mu}$ and $A_\lambda = \sum_\mu T_{\lambda\mu} A_\mu$. One changes $c$ to $c'$ in Eq. (8), multiplies by $\gamma_{\mu c}/(E_\mu - E)$, and sums over $\mu$ to obtain

$$\gamma_c = \sum_{c'\mu} \frac{\gamma_{\mu c'}\gamma_{\mu c} b_{c'}}{E_\mu - E} \sum_{\mu'} A_{\mu'}\gamma_{\mu'c'}, \tag{9}$$

or

$$\sum_{c'} [\delta_{cc'} - R_{cc'} b_{c'}]\gamma_{c'} = 0, \tag{10}$$

where

$$\gamma_c = \sum_\mu A_\mu \gamma_{\mu c}, \tag{11}$$

and

$$R_{cc'} = \sum_\mu \gamma_{\mu c}\gamma_{\mu c'}/(E_\mu - E). \tag{12}$$

The amplitudes are extracted from Eq. (9),

$$A_\mu = \frac{1}{E_\mu - E} \sum_c \gamma_{\mu c} b_c \gamma_c = \frac{1}{E_\mu - E} \sum_c \gamma_{\mu c} G_c(a_c). \tag{13}$$

A general solution for the coupled channels wave function in the external region is [1]

$$\Psi = \sum_c \left( \frac{x_c}{\sqrt{2k_c}} O_c + \frac{y_c}{\sqrt{2k_c}} I_c \right). \tag{14}$$

The collision matrix **S** provides an expression for the $x_c$ in terms of the $y_c$. In matrix notation,

$$\mathbf{x} = -\mathbf{S}\mathbf{y}. \tag{15}$$

From Eqs. (4), (6), (10), and (14), the fundamental $R$ matrix equation for the relativistic case relates the upper components of the wave functions to the lower,

$$F_c = \sum_{c'} R_{cc'} G_{c'} = \sum_{c'} R_{cc'} [G_{Oc'} x_{c'}/\sqrt{2k_{c'}} + G_{Ic'} y_{c'}/\sqrt{2k_{c'}}]$$

$$= F_{Oc} x_c/\sqrt{2k_c} + F_{Ic} y_c/\sqrt{2k_c}. \tag{16}$$

If one defines diagonal matrices $v_{cc'} = 2k_c\delta_{cc'}$, $x_{cc'} = \delta_{cc'}x_c$, $y_{cc'} = \delta_{cc'}y_c$, $G_{Occ'} = \delta_{cc'}G_{Oc}$, $G_{Icc'} = \delta_{cc'}G_{Ic}$, $F_{Occ'} = \delta_{cc'}F_{Oc}$, and $F_{Icc'} = \delta_{cc'}F_{Ic}$, this equation can be written as

$\mathbf{F_O}\mathbf{v}^{-1/2}\mathbf{x} + \mathbf{F_I}\mathbf{v}^{-1/2}\mathbf{y} = \mathbf{RG_O}\mathbf{v}^{-1/2}\mathbf{x} + \mathbf{RG_I}\mathbf{v}^{-1/2}\mathbf{y}$. If one solves for **x**, one obtains the form in Eq. (15), $x = -\mathbf{S}y$, where

$$\mathbf{S} = \mathbf{v}^{1/2}(\mathbf{Fo} - \mathbf{RGo})^{-1}(\mathbf{F_I} - \mathbf{RG_I})\mathbf{v}^{-1/2}. \tag{17}$$

Then the **T** matrix, $T_{cc'}$, is in the usual form, $i(\delta_{cc'} - S_{cc'})/2$.

The scattering amplitude is found by following standard techniques. Target (residual) states are noted as $|\alpha J_A M_A\rangle$, where $J_A$, $M_A$ are the spin and its projection and $\alpha$

distinguishes among states of the same spin. Target states may be coupled to the angular momentum of the projectile yielding states with total angular momentum and projection $|\alpha J_A \ell j J_B M_B\rangle$. The scattering states are designated by the target state, its projection, and the spin projection of the projectile $\sigma$. The resulting scattering amplitude is

$$\langle f \rangle_{\alpha \sigma M_A, \alpha' \sigma' M'_A}$$
$$= \frac{1}{k} \sum \sqrt{4\pi(2\ell+1)} C_{0\sigma m}^{\ell 1/2 j} C_{M_A m M_B}^{J_A j J_B} C_{M'_A m' M_B}^{J'_A j' J_B} C_{m'_\ell \sigma m'}^{\ell' 1/2 j'}$$
$$\times i^{(\ell-\ell')} e^{i(\delta'_\kappa + \delta'_{\kappa'})} T_{\alpha J_A \ell j J_B, \alpha' J'_A \ell' j' J'_B} Y_{\ell' m'_\ell}(\mathbf{k}'). \quad (18)$$

The sum is over $\kappa$, $\kappa'$, $\alpha'$, $J_B$, $M_B$, $m$, $m'$, and $m_{\ell'}$. Scattering observables can then be calculated from the scattering amplitude. For instance, the cross section would be given by

$$\frac{d\sigma}{d\Omega}(\theta) = \frac{1}{2(2J_A+1)} \sum_{\sigma\sigma' M'_A M_A} \big| \langle f_c \rangle_{\sigma\sigma'} \delta_{J_A \alpha M_A, J'_A \alpha' M'_A}$$
$$+ \langle f \rangle_{\alpha \sigma M_A, \alpha' \sigma' M'_A} \big|^2, \quad (19)$$

where $\langle f_c \rangle_{\sigma\sigma'}$ is the relativistic Coulomb scattering amplitude [5], taken to be diagonal in the target states.

## III. RELATIVISTIC CONTINUUM SHELL MODEL

The random-phase approximation and TDA equations for QHD were derived in Ref. [14] following Ref. [15] and appeared the same as the nonrelativistic equations. The TDA equation is

$$(\varepsilon_\lambda - \varepsilon_\mu - \varepsilon) C_{\lambda\mu} + \sum_{\alpha\beta} [\langle \beta\lambda|V|\alpha\mu\rangle - \langle \beta\lambda|V|\mu\alpha\rangle] C_{\alpha\beta} = 0. \quad (20)$$

To apply QHD to finite nuclei, the meson fields are taken as classical fields and a set of Dirac equations solved in the Hartree approximation [9,16]. The $\sigma$ and $\omega$ coupling constants were fit to the saturation properties of equilibrium nuclear matter, and the $\rho$ coupling constant was determined from the bulk symmetry energy. The $\sigma$ mass was determined so as to reproduce the rms radius of $^{40}$Ca, and for the Coulomb potential, one uses the contribution to the baryon density of protons only, whereas, for the $\rho$, one uses half the difference between the proton and the neutron densities. To implement the QHD results in a TDA equation, the classical meson fields are replaced with one-meson exchange potentials as in Ref. [14],

$$V = \frac{-g_\sigma^2}{4\pi} \frac{e^{-m_\sigma r}}{r} + \gamma_1^\lambda \gamma_{2\lambda} \frac{g_\omega^2}{4\pi} \frac{e^{-m_\omega r}}{r}$$
$$+ \gamma_1^\lambda \gamma_{2\lambda} \frac{\boldsymbol{\tau}_1 \cdot \boldsymbol{\tau}_2}{4} \frac{g_\rho^2}{4\pi} \frac{e^{-m_\rho r}}{r} + \gamma_1^0 \gamma_2^0 \frac{e^2}{r}, \quad (21)$$

where the Coulomb interaction has been included. The coupling constants employed are the same as those from QHD calculations, although it is not clear that these should be appropriate in structure calculations. The finite-Hartree (FH) coupling constants of Ref. [9] are shown in Table I. In addition, the hole SPEs, $\varepsilon_\mu$, and the wave functions are taken as those from the FH, QHD calculation, generated with the code TIMORA [16]. (A nucleon mass is added to the actual

TABLE I. Coupling constants. FH is finite Hartree; HF is Hartree-Fock.

| Meson | Mass (MeV) | FH, $g^2$ | HF, $g^2$ |
|---|---|---|---|
| $\sigma$ | 520 | 109.6 | 89.6 |
| $\omega$ | 783 | 190.4 | 102.6 |
| $\rho$ | 770 | 65.2 | 12.4 |
| $\pi$ | 138 | 0 | 181 |

output of the code to obtain $\varepsilon_\mu$.) However, the particle SPE, $\varepsilon_\lambda$, are replaced by the interaction of the particle with the core nucleons,

$$E_{jj} = \langle j|\boldsymbol{\alpha}\cdot\boldsymbol{p} + m\boldsymbol{\beta}|j'\rangle + \sum_{j_c, J}^{occ} \frac{2J+1}{2j+1} \langle \gamma_0 j \gamma_0 j_c(J)|V$$
$$\times [|j' j_c(J)\rangle - (-)^{j'+j_c-J}|j_c j'(J)\rangle], \quad (22)$$

where the sum $j_c$ is over proton and neutron states below the Fermi surface. The integrals extend only to the $R$ matrix radius. The notation is that $\langle \gamma_0 j|$ is $\bar{u} = u^+ \gamma_0$ with angular momentum $j$. A similar SPE definition could be made for the hole states with $|j\rangle$ and $|j'\rangle$ replaced with $|j_h\rangle$ giving $E_{j_h j_h}$.

Equation (20) is now an equation to be solved for the particle wave functions for a given energy. The basis functions, the $|\lambda\rangle$ of Eq. (3), are particle-hole functions where the $|j\rangle$ are Dirac oscillators specified by $|n\ell j\kappa\rangle$ and hole states are the QHD states generated with parameters FH as used to construct the targets in Ref. [5]. Hole states are the target states with spin $j_h = J_A$. A matrix element of the Hamiltonian (excluding the Bloch operator) within the $R$ matrix radius is

$$\langle j \otimes j_h(J_B)|H|j' \otimes j_{h'}(J_B)\rangle$$
$$= E_{jj'} - \varepsilon_{j_h} \delta_{j_h j_{h'}} - \sum_J (2J+1) W(j j_h j_{h'} j'; J_B J)$$
$$\times \langle \gamma_0 j_{h'} \gamma_0 j(J)|V[|j_h j(J)\rangle - (-)^{j_h+j-J}|j j_h(J)\rangle], \quad (23)$$

The particle wave functions are orthogonal to the hole states, and the exchange terms are calculated exactly in the method of Ref. [5].

To check whether replacing the classical fields with one-meson exchange potentials is appropriate, one can compare the single-particle energies of the hole states calculated from QHD and those calculated by the interaction of the hole state with particles in the core $E_{j_h j_h}$. The comparison is performed for two nuclei $^{16}$O and $^{90}$Zr. One is interested in $^{16}$O because it is the subject of numerous $(e,e'x)$ experiments and the question of the role of relativity in these reactions, however, only six SPEs can be compared for this nucleus. Therefore, a comparison is first made for $^{90}$Zr, which has 21 SPEs. The $^{90}$Zr comparison is shown in Table II for $E_{jj'}^x = E_{jj'} - M_N$. The first column lists the QHD output from TIMORA. The second column is from the one-pion exchange calculation with the same coupling constants. Although the SPEs calculated with the potential are shifted upward slightly and have some difficulties with the spin-orbit splitting, the agreement between the two calculations is surprising. In Table III is shown the SPE comparison for $^{16}$O where the agreement is similar. Also shown in this table are the experimental SPEs and those from a recent

TABLE II. Single-particle energies for $^{90}$Zr in MeV. Column 1 is the QHD finite-Hartree result; column 2 is the one-meson exchange with finite-Hartree parameters; column 3 is the same as column 2 plus pseudoscalar pions; column 4 is the same as column 2 plus pseudovector pions in the effective mass approximation; column 5 is the one-meson exchange with QHD Hartree-Fock parameters plus pseudoscalar pions.

| State | FH, QHD | FH, $E^x_{jj'}$ | FH, $E^x_{jj'}$ ps | FH, $E^x_{jj'}$ $M^*$ | HF, $E^x_{jj'}$ ps |
|---|---|---|---|---|---|
| $0s_{1/2}(p)$ | $-52.43$ | $-49.11$ | 37.17 | $-30.32$ | $-16.59$ |
| $0p_{3/2}(p)$ | $-42.06$ | $-40.32$ | 36.42 | $-20.99$ | $-14.24$ |
| $0p_{1/2}(p)$ | $-39.54$ | $-35.30$ | 47.47 | $-19.04$ | $-6.96$ |
| $0d_{5/2}(p)$ | $-30.15$ | $-29.96$ | 36.26 | $-10.33$ | $-9.99$ |
| $1s_{1/2}(p)$ | $-20.93$ | $-16.25$ | 52.86 | $-2.60$ | 3.22 |
| $0d_{3/2}(p)$ | $-24.86$ | $-19.88$ | 54.27 | $-6.56$ | 1.39 |
| $0f_{7/2}(p)$ | $-17.62$ | $-18.73$ | 36.54 | 0.52 | $-4.04$ |
| $1p_{3/2}(p)$ | $-6.92$ | $-2.54$ | 52.25 | 7.92 | 10.96 |
| $0f_{5/2}(p)$ | $-9.55$ | $-4.13$ | 57.14 | 5.99 | 9.17 |
| $1p_{1/2}(p)$ | $-5.11$ | 0.10 | 53.94 | 8.96 | 13.02 |
| $0s_{1/2}(n)$ | $-62.72$ | $-54.55$ | 30.44 | $-38.20$ | $-26.78$ |
| $0p_{3/2}(n)$ | $-51.04$ | $-44.17$ | 30.79 | $-27.80$ | $-23.70$ |
| $0p_{1/2}(n)$ | $-48.80$ | $-39.92$ | 42.77 | $-25.41$ | $-15.31$ |
| $0d_{5/2}(n)$ | $-38.18$ | $-32.82$ | 30.52 | $-16.53$ | $-19.40$ |
| $1s_{1/2}(n)$ | $-30.30$ | $-21.19$ | 45.05 | $-9.59$ | $-7.33$ |
| $0d_{3/2}(n)$ | $-33.20$ | $-23.53$ | 51.24 | $-11.64$ | $-5.49$ |
| $0f_{7/2}(n)$ | $-25.07$ | $-21.34$ | 30.02 | $-5.60$ | $-13.63$ |
| $1p_{3/2}(n)$ | $-15.94$ | $-7.84$ | 44.53 | 0.73 | 0.65 |
| $0f_{5/2}(n)$ | $-17.23$ | $-7.22$ | 54.56 | 1.67 | 3.03 |
| $1p_{1/2}(n)$ | $-14.03$ | $-4.94$ | 47.39 | 2.33 | 3.58 |
| $0g_{9/2}(n)$ | $-12.26$ | $-10.08$ | 29.53 | 4.27 | $-6.47$ |

nonrelativistic Hartree-Fock [17] calculation. These last two columns demonstrate that the original QHD, FH calculation has some difficulty with the spin-orbit splitting.

The $R$ matrix is now calculated for $^{16}$O, and the $R$ matrix level energies for $J^\pi = 2^-$ are plotted in Fig. 1. In a nonrelativistic calculation, one would have $R$ matrix levels below threshold corresponding to bound states, levels above threshold corresponding to resonances, and levels very much above threshold that comprise the continuum. These levels appear in the relativistic calculation as well, however, a nearly equal number of negative energy levels appear approximately one nucleon mass below threshold. These levels are absolutely necessary for the cross-sectional calculations.

In Fig. 2, the solid line represents the calculated 39.84-MeV elastic-scattering cross section for protons on $^{15}$N with the FH parameter set, the same set used to calculate the bound-state wave functions and bound-state SPEs. Hole states $|j_h\rangle$ are

limited to the $p$ shell, and their energies are taken as those from the QHD calculation. No pions are included in the FH interaction. The agreement with the data [18] is again surprisingly good. With only four core states, no absorption, and such a simple interaction, one does not expect the calculation to fit the backangle data. However, based on equivalent nonrelativistic calculations, one does expect a reasonable fit to forward angles, and this is accomplished. Included in Fig. 2 as a dotted line is the equivalent nonrelativistic calculation with the recoil corrected continuum shell model [19] and the
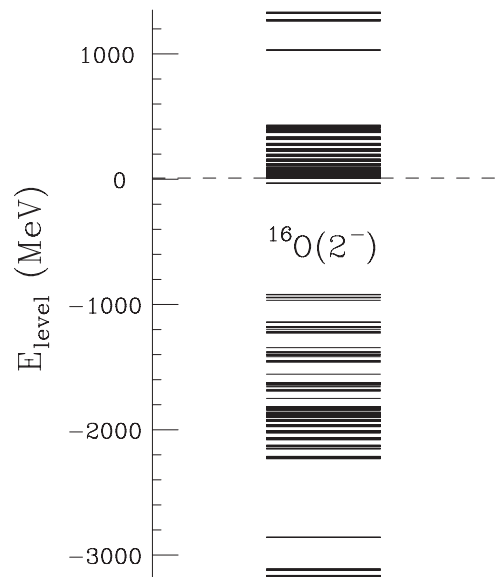
TABLE III. Single-particle energies for $^{16}$O in MeV. Column 1 is the QHD finite-Hartree result; column 2 is the one-meson exchange with finite-Hartree parameters; column 3 shows experimental values; column 4 shows results of a nonrelativistic Hartree-Fock calculation.

| State | FH, QHD | FH, $E^x_{jj'}$ | Exp. | Ref. [17] |
|---|---|---|---|---|
| $1s_{1/2}(p)$ | $-37.2$ | $-36.2$ | $-37 \pm 4$ | $-35.4$ |
| $1p_{3/2}(p)$ | $-16.7$ | $-17.8$ | $-17.4$ | $-18.6$ |
| $1p_{1/2}(p)$ | $-8.8$ | $-4.0$ | $-12.1$ | $-12.5$ |
| $1s_{1/2}(n)$ | $-41.4$ | $-39.0$ | $-40 \pm 4$ | $-38.6$ |
| $1p_{3/2}(n)$ | $-20.6$ | $-20.8$ | $-21.8$ | $-21.8$ |
| $1p_{1/2}(n)$ | $-12.5$ | $-6.7$ | $-15.7$ | $-15.6$ |



FIG. 1. $R$ matrix levels for $J^\pi = 2^-$.
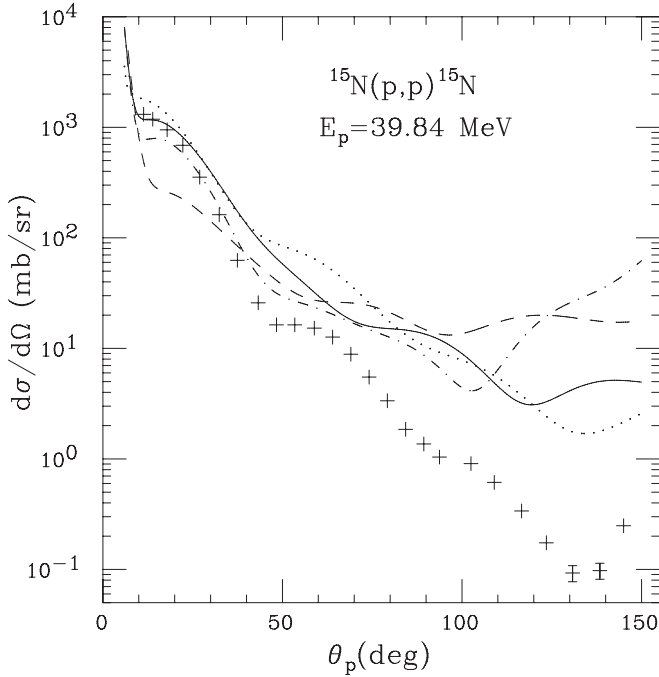
FIG. 2. Cross section for 39.84-MeV protons on $^{15}$N. The solid line uses FH parameters; the dashed line uses FH parameters plus pseudoscalar $\pi N$ coupling; the dot-dashed line uses effective mass approximation to pseudovector $\pi N$ coupling; the dotted line is nonrelativistic calculation. Data are from Ref. [15].

M3Y [20] interaction. The agreement with the data is about the same. The relativistic continuum shell model with the FH interaction is, therefore, a simple relatively self-consistent physically justified model in which to investigate relativistic contributions in knockout reactions.

## IV. PIONS

If one looks at the solid line in Fig. 2 as if it were scattering from a Woods-Saxon potential, one would consider altering the diffuseness to obtain a better fit. Indeed, QHD, FH has no pions whose longer range would alter the surface properties of an equivalent Woods-Saxon. Therefore, a brief look at the possible role of pions is worthwhile. The pions can be added by making the instantaneous approximation to the one-meson exchange propagator. In the case of pseudoscalar coupling, the energy transferred is set to zero, and $\Delta(x' - x) = \int \frac{d^4q}{(2\pi)^4} \frac{e^{-iq(x'-x)}}{k^2 - m_\pi^2 + i\varepsilon}$ becomes $- \int \frac{d^3q}{(2\pi)^3} e^{i\mathbf{k}\cdot(\mathbf{x}-\mathbf{x'})}/(k^2 + m_\pi^2 - i\varepsilon)\delta(t - t')$. The Fourier transform yields a Yukawa, and the term $\gamma_1^5 \gamma_2^5 \boldsymbol{\tau}_1 \cdot \boldsymbol{\tau}_2 \frac{g_\pi^2}{4\pi} \frac{e^{-m_\pi r}}{r}$ is added to Eq. (21). This approximation looks quite adequate if the energy transferred is reasonably small. However, the procedure is less satisfactory in the case of pseudovector coupling. The vertex function $(f_\pi/m_\pi)\gamma_5\displaystyle{\not}q\tau_i$ includes a term with the energy transferred. Setting this term to zero is very different than setting it to zero in the denominator of the propagator. However, a simple approximation was proposed in Ref. [14] in which pseudovector coupling is approximated by using an effective nucleon mass in the pseudoscalar matrix elements. The prescription is

that one uses the Yukawa interaction above, multiplied by $[M^*(\mathbf{x}_1)/M][M^*(\mathbf{x}_2)/M]$, where $M^* = M - g_S\varphi(r)$ and $g_S\varphi(r)$ is the scalar potential for the hole states. The effective mass approximation provides a density dependence for the interaction, although a severe one, the interior pion potential being reduced by approximately 75%.

The $^{15}$N $(p,p)$ $^{15}$N cross section with the FH coupling constants and pseudoscalar coupling with $g_\pi^2 = 181$ appears as a dashed line in Fig. 2. The cross section is more diffractive, but the fit is poor. This is reflected in the enormous increase in the $^{90}$Zr single-particle energies as shown in column 3 of Table II. This increase shows that, for these coupling constants, the pions are producing repulsion, just as they did in the Hartree-Fock calculations of QHD [9]. Also shown in Fig. 2, as a dot-dashed line, is the cross section with the effective mass approximation to pseudovector coupling. This addition has a smaller effect as one would expect from derivative coupling. It also improves the diffraction peak locations, but the severity of the density dependence produces unusual backangle behavior. The effective mass approximation produces the SPEs in column 4 of Table II, and they are certainly an improvement over the full pseudoscalar results. It is now clear why the structure calculations in Ref. [14] preferred this approximation to pseudovector coupling over pseudoscalar coupling.

Additional sets of coupling constants were obtained in the Hartree-Fock calculations of QHD, which included pions in the coupling constant fit [9]. The $\pi N$ coupling was pseudovector. One set of these coupling constants is given in Table I under the title HF. The SPE results of this representative set are shown in column 5 in Table II for pseudoscalar coupling. These SPEs are underbound. Use of the effective mass approximation to pseudovector coupling
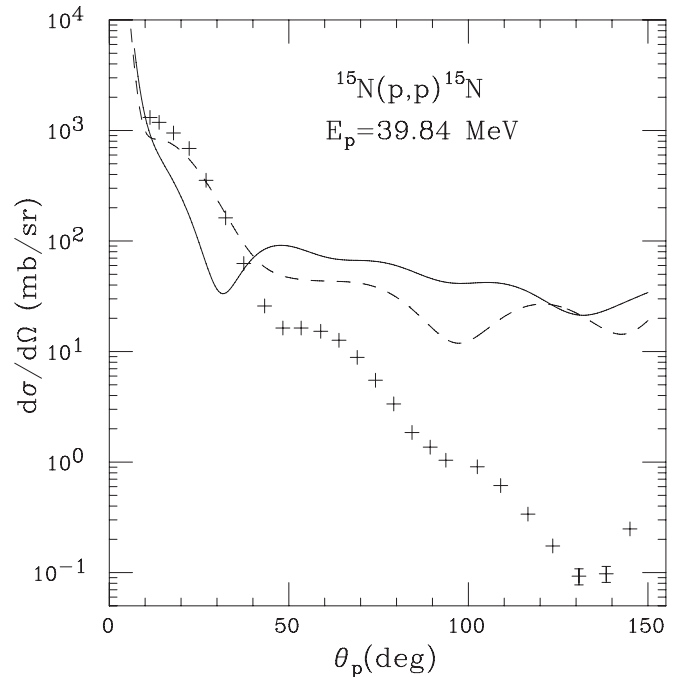


FIG. 3. Cross section for 39.84-MeV protons on $^{15}$N. The dashed line uses HF parameters plus pseudoscalar $\pi N$ coupling; the solid line is the same but without pions. Data are from Ref. [15].

produced extremely underbound SPEs and is considered unacceptable. The cross section with pseudoscalar coupling is shown as the dashed line in Fig. 3, and the cross section with no pions is shown as a solid line. The inclusion of the pions improves the cross section considerably, especially the location of the diffraction peaks, but the cross section still rises at backangles.

One can conclude that pions have the capability to alter the cross section, especially in a manner normally associated with surface effects. However, it would be very beneficial to have a better approximation for calculating the pseudovector matrix elements to adequately judge its effect.

## V. CONCLUSION

This paper provided the final derivations for a $R$ matrix formalism so that the many-coupled-channel problem may be solved for systems in which binary breakup channels satisfy a relative Dirac equation. Expressions for the collision matrix and the scattering amplitude are presented, and from these, one may calculate scattering observables. In addition to providing scattering states, this $R$ matrix formalism may also be used to calculate resonances and bound states.

The formalism is applied to relativistic continuum TDA calculations for $^{16}$O with interactions derived from relativistic mean-field theory. It was determined that even the simple $\sigma + \omega + \rho$ exchange with QHD coupling constants provides reasonable agreement with experimentally determined SPEs and the experimental $^{15}$N $(p,p)$ $^{15}$N cross section at 39.84 MeV. This is, therefore, a simple physically justifiable interaction for later use in knockout reactions.

[1] A. M. Lane and R. G. Thomas, Rev. Mod. Phys. **30**, 257 (1958).

[2] P. Descouvemont and D. Baye, Rep. Prog. Phys. **73**, 036301 (2010).

[3] D. Halderson, Int. J. Mod. Phys. E **14**, 171 (2005).

[4] D. Halderson, Nucl. Phys. A **487**, 647 (1988).

[5] J. Grineviciute and D. Halderson, Phys. Rev. C **80**, 044607 (2009).

[6] Ito, K. Mori and E. Carriere, Nuovo Cimento A **51**, 1119 (1967).

[7] M. Moshinsky and A. Szczepaniak, J. Phys. A **22**, L817 (1989).

[8] C. J. Horowitz, Phys. Rev. C **31**, 1340 (1985).

[9] B. D. Serot and J. D. Walecka, in *Advances in Nuclear Physics*, edited by J. W. Negele and E. Vogt (Plenum, New York, 1986), Vol. 16, p.1, and references therein.

[10] D. Halderson, Phys. Rev. C **53**, 2978 (1996).

[11] G. Young and P. H. Norrington, Comput. Phys. Commun. **83**, 215 (1994).

[12] J. Thompson and A. R. Barnett, Comput. Phys. Commun. **36**, 363 (1985).

[13] R. J. Philpott, Nucl. Phys. A **243**, 260 (1975).

[14] R. J. Furnstahl, Ph.D. dissertation, Stanford University, 1985; Phys. Lett. B **152**, 313 (1985).

[15] A. L. Fetter and J. D. Walecka, *Quantum Theory of Many-Particle Systems* (McGraw-Hill, New York, 1971), Chap. 15, p. 558.

[16] C. J. Horowitz, D. P. Murdock, and B. D. Serot, in *Computational Nuclear Physics*, edited by K. Langake, J. A. Maruhn, and S. E. Koonin (Springer Verlag, Berlin, 1991), Vol. 1, Chap. 7, p. 129.

[17] V. De Donno, G. Co, M. Anguiano, and A. M. Lallena, Phys. Rev. C **83**, 044324 (2011).

[18] J. L. Snelgrove and E. Kashy, Phys. Rev. **187**, 1259 (1969).

[19] D. Halderson and R. J. Philpott, Nucl. Phys. A **345**, 141 (1980).

[20] G. Bertsch, J. Borysowicz, H. McManus, and W. G. Love, Nucl. Phys. A **284**, 399 (1977), the interaction described on p. 412.